## **ARTICLE IN PRESS**

Applied Surface Science xxx (2017) xxx-xxx

EICEVIED

Contents lists available at ScienceDirect

### **Applied Surface Science**

journal homepage: www.elsevier.com/locate/apsusc



Full Length Article

# Thickness dependence of the electrical and thermoelectric properties of co-evaporated Sb<sub>2</sub>Te<sub>3</sub> films

Haishan Shen<sup>a,c</sup>, Suhyeon Lee<sup>c</sup>, Jun-gu Kang<sup>a</sup>, Tae-Yil Eom<sup>b</sup>, Hoojeong Lee<sup>a,\*</sup>, Seungwoo Han<sup>c,\*</sup>

- <sup>a</sup> Department of Advanced Materials Science and Engineering, Sungkyunkwan University, 2066, Seobu-ro, Jangan-gu, Suwon-si, 440-746, Republic of Korea
- <sup>b</sup> Division of Sungkyunkwan Advanced Institute of Nanotechnology (SAINT), Sungkyunkwan University, 2066, Seobu-ro, Jangan-gu, Suwon-si, 440-746, Republic of Korea
- <sup>c</sup> Division of Nano-Mechanical System Research, Korea Institute of Machinery & Materials, 156, Gajeongbuk-ro, Yuseong-gu, Daejeon-si, 305-343, Republic of Korea

#### ARTICLE INFO

Article history:
Received 31 March 2017
Received in revised form 11 August 2017
Accepted 5 September 2017
Available online xxx

Keywords: Anisotropic Mobility Recrystallization Thermoelectric Thickness

#### ABSTRACT

P-type antimony telluride ( $Sb_2Te_3$ ) films of various thicknesses (1-, 6-, 10-, and 16- $\mu$ m) were deposited on an oxidized Si (100) substrate at 250 °C by effusion cell co-evaporation. Microstructural analysis using X-ray diffraction, scanning electron microscopy, and transmission electron microscopy revealed that the grains of the films grew in a mode in which recrystallization was prevalent and grain growth subdued, in contrast to typical film growth, which is often characterized by grain growth. The resultant microstructure exhibited narrow columnar grains, the preferred orientation of which changed with film growth thickness from (1010) with the 1- $\mu$ m films to (015) for the 6- and 10- $\mu$ m films, and finally (110) for the 16- $\mu$ m films. Carrier mobility and the overall thermoelectric properties of the Sb<sub>2</sub>Te<sub>3</sub> films were affected significantly by changes in the film microstructure; this was attributed to the strong anisotropy of Sb<sub>2</sub>Te<sub>3</sub> regarding electrical conductivity. The highest power factor of 3.3 mW/mK² was observed for the 1- $\mu$ m-thick Sb<sub>2</sub>Te<sub>3</sub> film.

© 2017 Elsevier B.V. All rights reserved.

#### 1. Introduction

Global warming which causes serious climate change issue is mainly attributed i to the emission of carbon oxide (CO<sub>2</sub>). There are several ways to solve this issue. Likewise, using renewable energy, applying technologies for CO<sub>2</sub> capture and improving energy efficiency are becoming appealing [1–4]. One way to improve energy efficiency and waste heat recovery is through the use of thermoelectric (TE) material and devices which have the ability to convert thermal energy directly into electrical energy [5]. These materials are also used in wireless low-power devices, such as smart watches and hearing aids. Seiko and Citizen revealed watches driven by body heat, converted into electrical power by a micro-TE generator [6]. As devices become miniaturized, it is desirable to integrate micro-Peltier coolers into this microelectronics. An array of TE

E-mail addresses: hlee@skku.edu (H. Lee), swhan@kimm.re.kr (S. Han).

http://dx.doi.org/10.1016/j.apsusc.2017.09.037 0169-4332/© 2017 Elsevier B.V. All rights reserved. microdevices is commonly used for temperature stabilization to ensure optimal performance [7].

TE materials bismuth telluride ( $Bi_2Te_3$ ) and antimony telluride ( $Sb_2Te_3$ ) are widely used in near-room-temperature TE generator and Peltier cooler applications; these materials demonstrate the greatest figure of merit for both n- and p-type TE systems [5]. The figure of merit, i.e., the ability of a TE material to efficiently produce electricity, is given by

$$ZT = \alpha^2 T/\rho k$$

where T is the temperature,  $\alpha$  is the Seebeck coefficient,  $\rho$  is the electrical resistivity, and k is the thermal conductivity. Generally, TE materials are valued by the power factor  $(\alpha^2/\rho)$ . Previous research has shown that nanostructured thin films offer enhanced ZT values due to the enhanced Seebeck effect and reduced thermal conductivity [8]. Typically, 5- to 20- $\mu$ m-thick superlattice TE devices provide much higher heat flux pumping than 200- $\mu$ m-thick conventional bulk devices based on Bi<sub>2</sub>Te<sub>3</sub> alloys [9].

Hence, nanostructured TE film structures have gained considerable attention in the research community. There have been several studies on tellurium-based materials and TE power performance as it relates to film composition [10,11], microstructure [12,13],

<sup>\*</sup> Corresponding authors at: 2066, Seobu-ro, Jangan-gu, Suwon-si, 440-746, Republic of Korea and 156, Gajeongbuk-ro, Yuseong-gu, Daejeon-si, 305-343, Republic of Korea.

H. Shen et al. / Applied Surface Science xxx (2017) xxx-xxx

**Table 1**Deposition condition of films.

Film	Substrate temperature (°C)	Ratio = $R_{Te}/R_{Sb}$	Deposited time (min)	Thickness (µm)
1	250	2.6	40	1
2	250	2.6	198	6
3	250	2.6	330	10
4	250	2.6	500	16

the grain boundary interface [14,15], and film thickness [16–18]; however, these studies focused on nanometer-sized thin films. Few studies have examined the properties of TE thin films with thicknesses of the order of microns.

In this study, the TE properties of p-type micron-thick  $\mathrm{Sb}_2\mathrm{Te}_3$  thin films were examined in an attempt to improve TE power performance. Several films of varying thickness (1-, 6-, 10-, and 16- $\mu$ m-thick) were prepared on a  $\mathrm{Si}(100)$  substrate at  $250\,^{\circ}\mathrm{C}$  by effusion cell co-evaporation. X-ray diffraction (XRD), scanning electron microscopy (SEM), and transmission electron microscopy (TEM) measurements were performed to resolve the thickness effect on recrystallization, grain growth, and TE performance.

#### 2. Experimental

#### 2.1. Sample preparation

Antimony telluride (Sb<sub>2</sub>Te<sub>3</sub>) films with different thicknesses were grown using the Ap-ece-150 co-evaporation model (Alphaplus, Co., Ltd., Pohang, Korea). Before film deposition, Si (100) wafers covered by a 300-nm-thick SiO<sub>2</sub> layer were cleaned sequentially in isopropyl alcohol, acetone, and methanol in an ultrasonic bath for 5 min and then rinsed with deionized water. The substrates were then exposed to O<sub>2</sub> plasma for 30 s to remove the organic solution. High-purity Sb (99.9999%) and Te (99.9999%) sources were prepared and evaporated by effusion cells, allowing precise temperature control. The Sb evaporation flow rate (R<sub>Sb</sub>) was set at  $1.5 \,\text{Å/s}$  whereas Te evaporation flow rate ( $R_{Te}$ ) was maintained at 3.9 Å/s. The evaporation flow ratio ( $R = R_{Te}/R_{Sh}$ ) is 2.6, defined as the evaporation flow rate of Te divided by evaporation flow rate of Sb. To obtain precise composition of film, controlling the evaporation flow ratio is important. The pressure of the evaporator system during deposition was maintained below  $5 \times 10^{-7} \, \text{Torr.}$ During film fabrication, the Si substrate was rotated at 4 rpm for uniform film deposition; a 300-nm-thick oxidation layer of silicon wafer provided electrical and thermal insulation. The time for each film deposition experiment was varied to obtain different thicknesses. It has been reported that film growth at higher deposition temperature have improved crystallinity due to enhanced surface diffusion and clustering of adatoms at higher temperature [19]. For this reason, the deposition temperature was fixed at 250 °C. Table 1 lists the film thicknesses and deposition conditions for each sample.

#### 2.2. Characterization

The XRD measurements were carried out at 45 kV and 30 mA with an X'Pert-MPD (PANalytical) diffractometer (Phillips, Best, The Netherlands) using Cu-K $\alpha_1$  radiation ( $\lambda$  = 1.5406 Å), whereby the diffraction angle was varied from 10° to 65°. The surface, cross-sectional morphology, and thickness of each film were investigated by field-emission scanning electron microscopy (FE-SEM) (Tescan Lyra 3; Tescan, Brno, Czech). Film composition was evaluated using energy dispersive X-ray spectroscopy (EDS; operating voltage: 15 kV) via an Oxford X-Max (Oxford Instruments, Oxford, UK). TEM (JEOL JEM-2100F) provided information on the film microstructure. The electrical properties of the films were measured by a Hall-effect

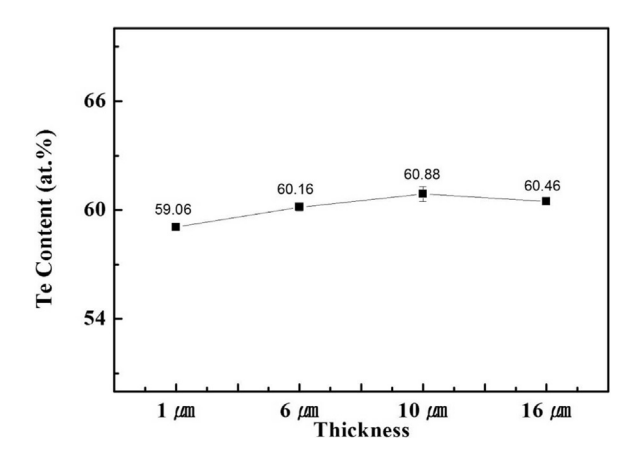


Fig. 1. Te content of the 1-, 6-, 10-, and 16- µm-thick Sb<sub>2</sub>Te<sub>3</sub> films.

measurement system (HMS-5000, ECOPIA, Chandler Hall, AZ, USA), operating at room temperature. Van der Pauw measurements (1-mA direct current; magnetic field strength: 0.55 T) were used to obtain the carrier concentration, carrier mobility, and film resistivity. The room temperature Seebeck coefficient was measured using Fraunhofer IPM-RT system (Fraunhofer, Freiburg, Germany). The temperature gradient over the samples and the generated thermopower voltage were measured with two type T thermocouples. The measurement was carried out twice for each sample: While heating one side of the sample (side A), the increasing temperature gradient and thermopower voltage was measured. Then, the other side (side B) was heated and the Seebeck coefficient was obtained in a similar way. We used the average value of the two values for this study. The power factor was calculated from the electrical resistivity and Seebeck coefficient.

#### 3. Results and discussion

Fig. 1 shows the tellurium compositions for films of different thicknesses, determined by energy dispersive X-ray spectroscopy (EDS) during field-emission scanning electron microscopy (FE-SEM) operation. While the film thickness varies quite widely from 1  $\mu$ m to 16  $\mu$ m, the film composition remains nearly the same. In addition, the film composition is close to the Sb<sub>2</sub>Te<sub>3</sub> stoichiometry. It is known that the Sb-Te films of the stoichiometric composition exhibits maximum power factor [20].

Fig. 2 shows X-ray diffraction (XRD) patterns for the films. As expected, the peak intensity grew markedly with increasing film thickness; an interesting aspect of the data is that while the overall peak intensity differed among film samples, careful examination revealed a systematic shift in the dominant peaks with thickness. For a better comparison, we replotted the data at different scales for each sample, as shown in Fig. 2b. For the 1- $\mu$ m-thick film, the (1010) showed the dominant peak intensity. As the thickness of the films increased to 6 and 10  $\mu$ m, the (015) peak, the main peak of antimony telluride (Sb<sub>2</sub>Te<sub>3</sub>), became stronger [21]. For the 16- $\mu$ m-thick film sample, the film texture changed from (015) to (110). Thus, during film growth, the film texture changed from (1010) to (015) and then to (110).

Fig. 3 shows top- and cross-sectional views of FE-SEM images of  $Sb_2Te_3$  films for the 1-, 6-, 10-, and 16- $\mu$ m-thick film samples, in which the grain morphology was revealed. In the images, granular morphology was evident on the top surface, whereas the cross-sectional view showed a columnar morphology. Additionally, the morphology size increased significantly with an increase in film thickness from 1 to 6  $\mu$ m, indicating typical grain growth [18]. However, it is interesting to note that the increase was markedly subdued for film growth beyond 6- $\mu$ m thickness.

Please cite this article in press as: H. Shen, et al., Thickness dependence of the electrical and thermoelectric properties of co-evaporated  $Sb_2Te_3$  films, Appl. Surf. Sci. (2017), http://dx.doi.org/10.1016/j.apsusc.2017.09.037

#### Download English Version:

## https://daneshyari.com/en/article/7836819

Download Persian Version:

https://daneshyari.com/article/7836819

<u>Daneshyari.com</u>